

# Design, Synthesis, Application, and DFT Investigation of Suzuki–Miyaura Reactions of a Dicobalt Carbonyl-Containing Phosphine Ligand

Yu-Chang Chang, Jian-Cheng Lee, and Fung-E. Hong\*

Department of Chemistry, National Chung-Hsing University, Taichung 40227, Taiwan

Received January 30, 2005

The preparation and characterization of a novel dicobalt-containing monophosphine ligand, **4a**, is presented. Palladium-catalyzed Suzuki–Miyaura reactions employing **4a**/Pd(OAc)<sub>2</sub> were pursued. The optimized reaction conditions were found to start with 1 molar equiv of arylhalides, 1.5-fold of phenylboronic acid, 3-fold of KF in 1 mL of THF, and 1 mol % of **4a**/Pd(OAc)<sub>2</sub> as catalytic precursor. The <sup>31</sup>P NMR studies reveal moderate reductive capacity of **4a** toward Pd(OAc)<sub>2</sub>. The unique bonding mode of **4a** toward Pd ensures that the ratio of **4a**/Pd is equal to 1:1. Two plausible active species, **I** and [**I-OAc**]<sup>-</sup>, were proposed as the catalytically active species in the Suzuki–Miyaura cross-coupling reaction. The validity of this assumption was examined by <sup>31</sup>P NMR spectra and density functional theory (DFT) means. In addition, we have demonstrated theoretically that the dicobalt moiety of **4a** acts as an effective auxiliary in stabilizing the Pd(0) center during catalytic reaction.

## 1. Introduction

The Suzuki–Miyaura reaction<sup>1</sup> is one of the most versatile catalytic cross-coupling reactions that comprise C–C, C–H, C–N, C–O, C–S, C–P, or C–M bond formation.<sup>2</sup> Most of the reactions employ phosphine-assisted palladium complexes as catalytic precursors. As known, a phosphine with both the characteristics of bulkiness and electron-richness not only accelerates the rate of oxidative addition of arylhalide to Pd(0)L<sub>n</sub> (L: phosphine; n = 1–2) but also speeds up the process of the reductive elimination of diaryl from the Pd(II) center.<sup>3,4</sup>

Although various synthetic methods have been explored in search of more versatile and efficient organic phosphines for the palladium/phosphine-catalyzed Su-

zuki–Miyaura cross-coupling reactions,<sup>5</sup> to our best knowledge, a systematical investigation of transition-metal-containing phosphines (TM-phosphines) has yet remained a relatively uncultivated land.<sup>6,7</sup> Three categories of TM-phosphines, which have been reported with appreciable efficiencies in Suzuki–Miyaura reactions, are depicted in Figure 1 according to their organometallic backbones. The common features that make these phosphines attractive are as follows: (1) easy to prepare with satisfactory yield; (2) stable toward air and therefore easy to handle; (3) adjustable bulkiness. It is noteworthy that all the metal centers in these three kinds of phosphines play the role of “spectator”. This affects the catalytic efficiency only via indirect means such as electron-withdrawing/donating and steric effects rather than forming a direct metal–substrate bond.<sup>7a,8</sup> Despite the limitation, these modifiable, bulky metal-containing substituents are undoubtedly one of the most unique features of these types of ligands.

The authors of this paper here contribute a new category of metal-containing phosphine ligands that will allow us to access straightforwardly a family of phos-

\* To whom correspondence should be addressed. Fax: (+886) 2-04-22862547. E-mail: fehong@dragon.nchu.edu.tw.

(1) (a) Suzuki, A. In *Metal-Catalyzed Cross-coupling Reactions*; Diederich, F.; Stang, P. J. Eds.; Wiley-VCH: Weinheim, Germany, 1998; Chapter 2. (b) Miyura, N.; Suzuki, A. *Chem. Rev.* **1995**, *95*, 2457–2483. (c) Suzuki, A. *J. Organomet. Chem.* **1999**, *576*, 147–168.

(2) General reviews, see: (a) Cross-Coupling Reactions—A Practical Guide. In *Topics in Current Chemistry*; Houk, K. N.; Sessler, H.; Lehn, J.-M.; Ley, S. V.; De Meijere, A.; Schreiber, S. L.; Thiem, J.; Trost, B. M.; Vögtle, F.; Yamamoto, H., Eds.; Springer-Verlag: Heidelberg, 2002; Vol. 219. (b) Hegedus, L. S. In *Organometallics in Organic Synthesis*; Schlosser, M., Eds.; Wiley: New York, 1994; p 383. (c) *Palladium Reagents and Catalysts: Innovations in Organic Synthesis*; Fuji, J., Eds.; Wiley: Chichester, 1995. (d) Geissler, H. In *Transition Metals for Organic Synthesis*; Beller, M.; Bolm, C., Eds.; Wiley-VCH: Weinheim, 1998; Vol. 1, pp 158–193. (e) *Metal-Catalyzed Cross-coupling Reactions*; Diederich, F.; Stang, P. J., Eds.; Wiley-VCH: Weinheim, Germany, 1998. (f) *Palladium in Heterocyclic Chemistry: A Guide for the Synthetic Chemist*; Li, J. J.; Gribble, G. W., Eds.; Pergamon: Amsterdam, 2000.

(3) (a) Chemler, S. R.; Trauner, D.; Danishefsky, S. J. *Angew. Chem., Int. Ed.* **2001**, *40*, 4544–4568. (b) Wolfe, J. P.; Tomori, H.; Sadighi, J. P.; Yin, J.; Buchwald, S. L. *J. Org. Chem.* **2000**, *65*, 1158–1174. (c) Wolfe, J. P.; Buchwald, S. L. *Angew. Chem., Int. Ed.* **1999**, *38*, 2413–2416. (d) Wolfe, J. P.; Singer, R. A.; Yang, B. H.; Buchwald, S. L. *J. Am. Chem. Soc.* **1999**, *121*, 9550–9561. (e) Bei, X.; Crevier, T.; Guram, A. S.; Jandeleit, B.; Powers, T. S.; Turner, H. W.; Uno, T.; Weinberg, W. H. *Tetrahedron Lett.* **1999**, *40*, 3855–3858. (f) Littke, A. F.; Fu, G. C. *Angew. Chem., Int. Ed.* **1998**, *37*, 3387–3388.

(4) (a) Littke, A. F.; Dai, C.; Fu, G. C. *J. Am. Chem. Soc.* **2000**, *122*, 4020–4028. (b) Zapf, A.; Ehrentraut, A.; Beller, M. *Angew. Chem., Int. Ed.* **2000**, *39*, 4153–4155. (c) Clarke, M. L.; Cole-Hamilton, D. J.; Woolins, J. D. *Dalton Trans.* **2001**, 2721–2723. (d) Li, G. Y. *J. Org. Chem.* **2002**, *67*, 3643–3650.

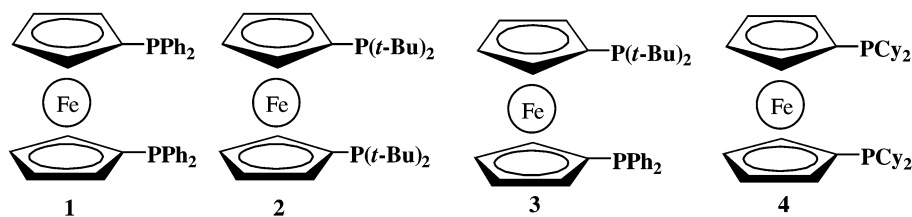
(5) Miura, M. *Angew. Chem., Int. Ed.* **2004**, *43*, 2201–2203.

(6) General reviews, see: (a) Delacroix, O.; Gladysz, J. A. *Chem. Commun.* **2003**, 665–675. (b) Salzer, A. *Coord. Chem. Rev.* **2003**, *242*, 59–72.

(7) (a) Planas, J. G.; Gladysz, J. A. *Inorg. Chem.* **2002**, *41*, 6947–6949. (b) Hu, Q.-S.; Lu, Y.; Tang, Z.-Y.; Yu, H.-B. *J. Am. Chem. Soc.* **2003**, *125*, 2856–2857. (c) Mann, G.; Hartwig, G. F. *J. Am. Chem. Soc.* **1996**, *118*, 13109–13110. (d) Pickett, T. E.; Roca, F. X.; Richards, C. J. *J. Org. Chem.* **2003**, *68*, 2592–2599. (e) Kataoka, N.; Shelby, Q.; Stambuli, J. P.; Hartwig, J. F. *J. Org. Chem.* **2002**, *67*, 5553–5566. (f) Tang, Z.-Y.; Lu, Y.; Hu, Q.-S. *Org. Lett.* **2003**, *5*, 297–300. (g) Jesen, J. F.; Johannsen, M. *Org. Lett.* **2003**, *5*, 3025–3028.

(8) (a) Zwick, B. D.; Arif, A. M.; Patton, A. T.; Gladysz, J. A. *Angew. Chem., Int. Ed. Engl.* **1987**, *26*, 910–912. (b) Planas, J. G.; Gladysz, J. A. *Inorg. Chem.* **2002**, *41*, 6947–6949.

## Group I: Ferrocene based di-phosphine ligands



## Group II: Ferrocene based mono-phosphine ligands

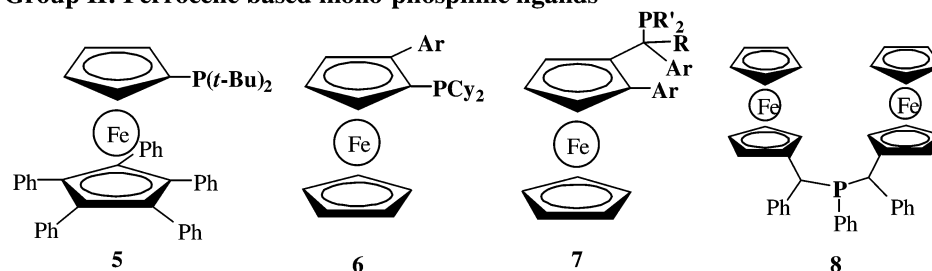
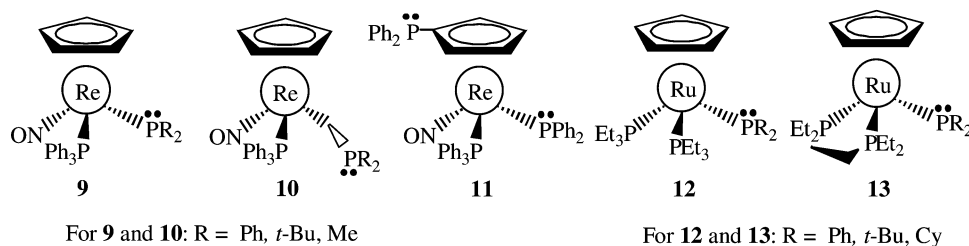
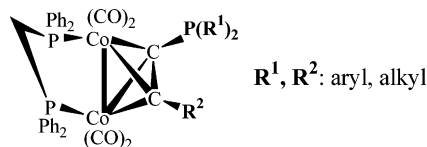
Group III: Phosphine ligands of  $L_nMPR_2$ 

Figure 1.

## Chart 1



phines with bulkiness and hopefully electron-richness. Extending from our current interest in alkyne-bridged dicobalt skeleton  $(Co_2(CO)_6(\mu-R^1C\equiv CR^2))$  systems,<sup>9</sup> a new series of novel cobalt-containing (mono- or di-) TM-phosphines has been developed and their catalytic efficiencies in phosphine-modified, palladium-catalyzed Suzuki–Miyaura reactions were evaluated (Chart 1). In recent DFT studies on the  $PPh_3/Pd(OAc)_2$ -catalyzed cross-coupling reactions,<sup>10</sup> a three-coordinate anionic  $[(PPh_3)_2Pd^0(OAc)]^-$  was proposed as the catalytically active species.<sup>11</sup> In the studies, they also proposed that

(9) (a) Dickson, R. S. *Adv. Organomet. Chem.* **1974**, *12*, 323–377. (b) Caffyn, A. J. M.; Nicholas, K. M. in *Comprehensive Organometallic Chemistry II*; Abel, E. W.; Stone, F. G. A.; Wilkinson, G., Eds.; Elsevier Science Inc.: New York, 1995; Vol. 12, p 685. (c) Schore, N. E. in *Comprehensive Organometallic Chemistry II*; Abel, E. W.; Stone, F. G. A.; Wilkinson, G., Eds.; Elsevier Science Inc.: New York, 1995; Vol. 12, p 703. (d) Templeton, J. L. in *Advances in Organometallic Chemistry*; Stone, F. G. A.; West, R., Eds.; Academic Press Inc.: New York, 1989; Vol. 29, p 1. (e) Lukehart, C. M. in *Fundamental Transition Metal Organometallic Chemistry*; Monterey, C., Ed.; Brooks/Cole, 1985. (f) Chetcuti, M. J. in *Comprehensive Organometallic Chemistry II*; Abel, E. W.; Stone, F. G. A.; Wilkinson, G., Eds.; Elsevier Science Inc.: New York, 1995; Vol. 10, p 23.

(10) (a) Goossen, L. J.; Koley, D.; Hermann, H. L.; Thiel, W. *Organometallics* **2004**, *23*, 2398–2410. (b) Kozuch, S.; Shaik, S.; Jutand, A.; Amatore, C. *Chem. Eur. J.* **2004**, *10*, 3072–3080.

(11) Amatore, C.; Jutand, A.; M'Barki, M. A. *Organometallics* **1992**, *11*, 3009–3013.

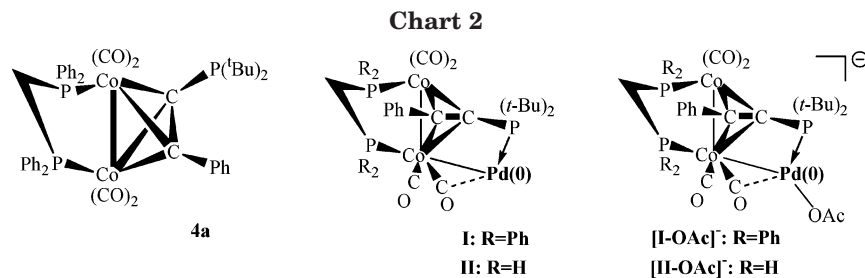
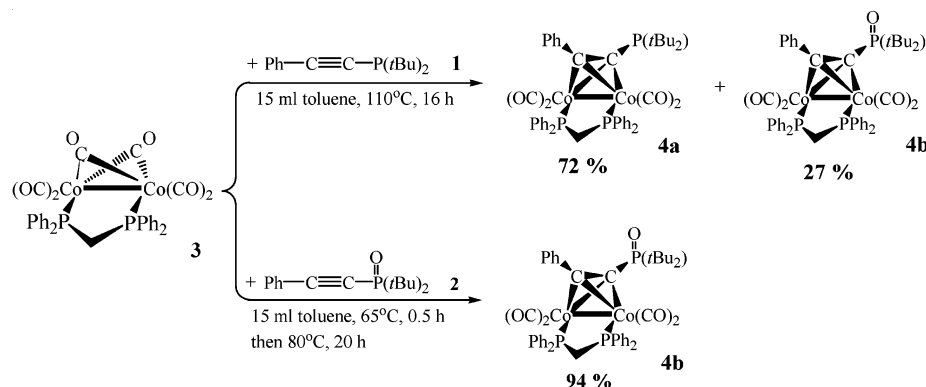
phosphine plays the role in reducing the Pd(II) to Pd(0) species. Hayashi et al. reported the effective reducing capacity of (*R*)-BINAP ((*R*)-2,2'-bis(diphenylphosphino)-1,1'-binaphthyl) toward  $Pd(OAc)_2$ . Accompanied with the reduction of Pd(II) to Pd(0), one of the phosphino sites of BINAP was oxidized.<sup>12</sup> This experimental result provides direct evidence of the production of a catalytically active Pd(0) complex from Pd(II) by a bulky phosphine. As known, the organoborane is also a capable reducing agent besides phosphine in Suzuki–Miyaura reactions.<sup>13</sup>

In this study, the preparation of a TM-phosphine,  $[(\mu-PPh_2CH_2PPh_2)Co_2(CO)_4][\mu,\eta-PhC\equiv CP(t-Bu)_2]$  (**4a**), an organometallic version of di-*tert*-butylphosphine, and its applications in a phosphine-modified, palladium-catalyzed cross-coupling reactions are presented. A moderate reducing capacity of **4a** toward Pd(II) will also be demonstrated later. This occurred through stoichiometric reduction of Pd(II) to Pd(0) by **4a** and was monitored in situ by <sup>31</sup>P NMR spectra. Two potential catalytically active species, **I** and  $[I-OAc]^-$ , involved in the catalytic reaction are proposed. By the way, the anionic species  $[I-OAc]^-$  analogue  $[(PPh_3)_2Pd^0(OAc)]^-$  was studied extensively by Jutand and Shaik et al.<sup>14</sup> To explicate the structures of **I** and  $[I-OAc]^-$ , DFT studies on two simplified model compounds, **II** and  $[II-OAc]^-$ , were pursued. Structural comparison between the theoretic-

(12) Ozawa, F.; Kubo, A.; Hayashi, T. *Chem. Lett.* **1992**, 2177–2180.

(13) Mareno-Manãs, M.; Pérez, M.; Pleixats, R. *J. Org. Chem.* **1996**, *61*, 2346–2351.

(14) Kozuch, S.; Amatore, C.; Jutand, A.; Shaik, S. *Organometallics* **2005**, *24*, 2319–2330.

**Scheme 1****Table 1. Crystal Data of 3 and 4a**

	<b>3</b>	<b>4a</b>
formula	C <sub>3</sub> H <sub>22</sub> Co <sub>2</sub> O <sub>6</sub> P <sub>2</sub>	C <sub>45</sub> H <sub>45</sub> Co <sub>2</sub> O <sub>4</sub> P <sub>3</sub>
fw	670.29	860.58
cryst syst	monoclinic	monoclinic
space group	P2(1)/n	P2(1)/n
<i>a</i> (Å)	10.4249(8)	14.0309(9)
<i>b</i> (Å)	13.7370(11)	18.7606(12)
<i>c</i> (Å)	20.5729(15)	16.4738(11)
$\beta$ (deg)	92.199(2)	91.1690(10)
<i>V</i> (Å <sup>3</sup> )	2944.0(4)	4335.5(5)
<i>Z</i>	4	4
<i>D<sub>c</sub></i> (Mg/m <sup>3</sup> )	1.512	1.672
$\lambda$ (Mo K $\alpha$ ) (Å)	0.71073	0.71073
$\mu$ (mm <sup>-1</sup> )	1.278	0.916
2 $\theta$ range (deg)	1.78 to 26.02	1.81 to 26.02
no. of obsd reflns ( <i>F</i> > 4 $\sigma$ ( <i>F</i> ))	5990	7931
no. of refined params	370	487
R1 for significant reflns <sup>a</sup>	0.0319	0.0352
wR2 for significant reflns <sup>b</sup>	0.0782	0.0877
GoF <sup>c</sup>	0.966	0.952

<sup>a</sup> R1 =  $\{\sum(|F_o| - |F_c|)/\sum F_o\}$ , <sup>b</sup> wR2 =  $\{\sum[w(F_o^2 - F_c^2)]^2/\sum[w(F_o^2)]^2\}^{1/2}$ ; *w* = 0.0499 and 0.0561 for **3** and **4a**. <sup>c</sup> GoF =  $[\sum w(F_o^2 - F_c^2)^2/(N_{\text{reflns}} - N_{\text{params}})]^{1/2}$ .

cally predicted geometries and the experimentally observed structures was described (Chart 2). On the basis of the previous calculations, the process of the generation of the monoligated palladium species as the active catalyst is thereby postulated.<sup>15</sup>

## 2. Results and Discussion

### 2.1. Preparation of a Dicobalt-Containing Phosphine Ligand, 4a. Our previous works have demon-

strated the unique character of a number of dicobalt-containing mono-<sup>16</sup> and diphosphine<sup>17</sup> ligands in palladium-catalyzed cross-coupling reactions. During the course of searching for more versatile and efficient phosphine ligands, we were attracted by two of the most efficient organic phosphine ligands: 2-(di-*tert*-butylphosphino)biphenyl and tri-*tert*-butylphosphine. The bulky substitutes and electron-donating ability of *tert*-butyl groups are believed to play a vital role in the processes of oxidative addition, transmetalation, and reductive elimination. Consequently, an organometallic version of

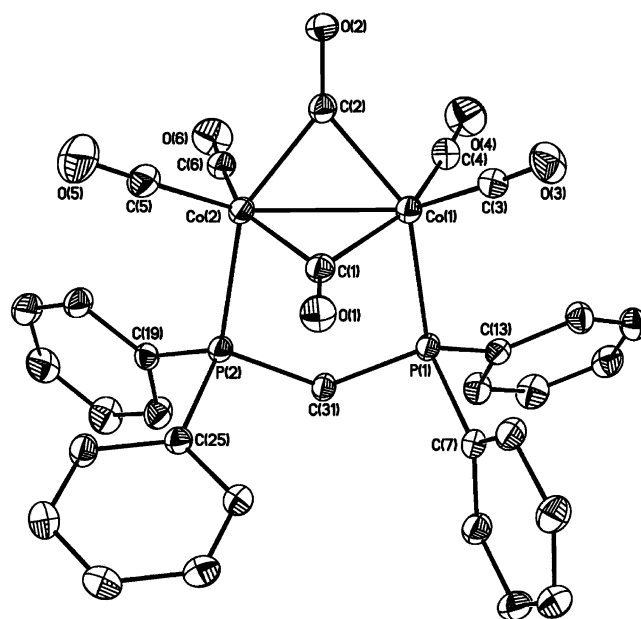


**Figure 2.** Molecular structure of  $(\mu\text{-PPh}_2\text{CH}_2\text{PPh}_2)\text{Co}_2(\text{CO})_6$ , **3**. Hydrogen atoms are omitted for clarity. Selected bond lengths (Å) and angles (deg): Co(1)–Co(2) 2.4568(5), Co(1)–P(1) 2.2658(7), Co(2)–P(2) 2.2388(7), Co(1)–C(1) 1.953(3), Co(1)–C(2) 1.946(3), Co(2)–C(1) 1.933(3), Co(2)–C(2) 1.921(3), P(1)–Co(1)–Co(2) 97.27(2), P(2)–Co(2)–Co(1) 99.96(2), P(2)–C(31)–P(1) 115.92(13).

(15) Christmann, U.; Vilar, R. *Angew. Chem., Int. Ed.* **2005**, *44*, 366–374.

(16) (a) Hong, F.-E.; Ho, Y.-J.; Chang, Y.-C.; Lai, Y.-C. *Tetrahedron* **2004**, *60*, 2639–2645. (b) Hong, F.-E.; Chang, C.-P.; Chang, Y.-C. *Dalton Trans.* **2003**, 3892–3897. (c) Hong, F.-E.; Lai, Y.-C.; Ho, Y.-J.; Chang, Y.-C. *J. Organomet. Chem.* **2003**, *688*, 161–167.

(17) (a) Hong, F.-E.; Chang, Y.-C.; Chang, C.-P.; Huang, Y.-L. *Dalton Trans.* **2004**, 157–165. (b) Hong, F.-E.; Chang, Y.-C.; Chang, R.-E.; Chen, S.-C.; Ko, B.-T. *Organometallics* **2002**, *21*, 961–967.



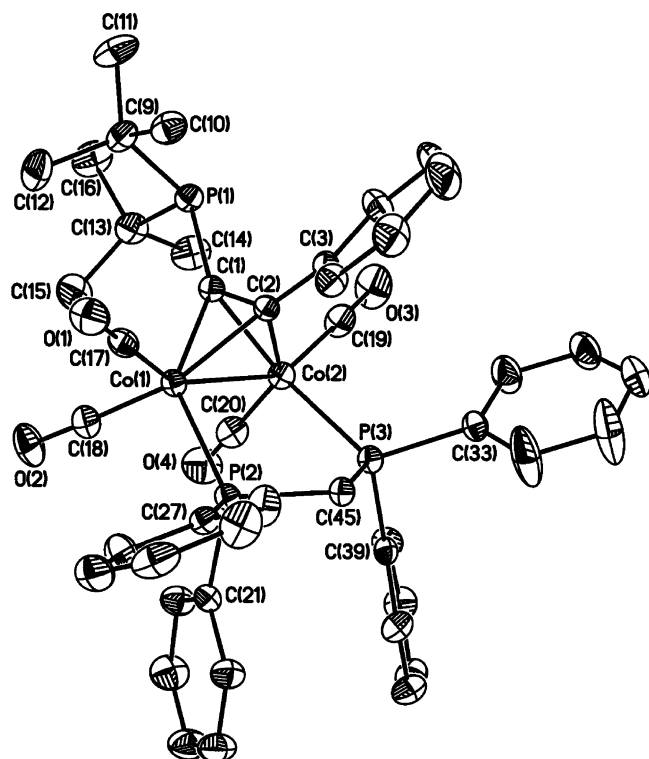


**Figure 3.** Molecular structure of  $[(\mu\text{-PPh}_2\text{CH}_2\text{PPh}_2)\text{Co}_2(\text{CO})_4(\mu,\eta\text{-PhC}\equiv\text{CP}(t\text{Bu})_2)]$ , **4a**. Hydrogen atoms are omitted for clarity. Selected bond lengths (Å) and angles (deg): Co(1)–Co(2) 2.4906(5), Co(1)–P(2) 2.2322(7), Co(2)–P(3) 2.2343(7), Co(1)–C(1) 2.009(2), Co(1)–C(2) 1.955(2), Co(2)–C(1) 1.983(2), Co(2)–C(2) 1.965(2), P(1)–C(1) 1.811(2), P(2)–Co(1)–Co(2) 92.86(2), P(3)–Co(2)–Co(1) 98.75(2), P(3)–C(45)–P(2) 109.71(12).

2-(di-*tert*-butylphosphino)biphenyl, TM-phosphine  $[(\mu\text{-PPh}_2\text{CH}_2\text{PPh}_2)\text{Co}_2(\text{CO})_4][\mu,\eta\text{-PhC}\equiv\text{CP}(t\text{Bu})_2]$  (**4a**), was prepared by the procedures as shown (Scheme 1).

First, two alkynyl phosphines,  $\text{PhC}\equiv\text{CP}(t\text{Bu})_2$  (**1**) and  $\text{PhC}\equiv\text{CP}(=\text{O})(t\text{Bu})_2$  (**2**), were synthesized by the procedures modified from the literature.<sup>18</sup> Further treatment of a DPPM-bridged dicobalt compound  $[\text{Co}_2(\text{CO})_6(\mu\text{-P,P-PPh}_2\text{CH}_2\text{PPh}_2)]$  (**3**) with 1 molar equiv of alkynyl phosphines  $\text{PhC}\equiv\text{CP}(t\text{Bu})_2$  (**1**) in toluene at 110 °C afforded the alkyne-bridged dicobalt compound  $[(\mu\text{-PPh}_2\text{CH}_2\text{PPh}_2)\text{Co}_2(\text{CO})_4][\mu,\eta\text{-PhC}\equiv\text{CP}(t\text{Bu})_2]$  (**4a**) and a small amount of oxidized  $[(\mu\text{-PPh}_2\text{CH}_2\text{PPh}_2)\text{Co}_2(\text{CO})_4][\mu,\eta\text{-PhC}\equiv\text{CP}(=\text{O})(t\text{Bu})_2]$  (**4b**). The latter compound can also be prepared directly from the reaction of **3** with  $\text{PhC}\equiv\text{CP}(=\text{O})(t\text{Bu})_2$  (**2**). Both **4a** and **4b** were characterized by spectroscopic means, and the crystal structure of **4a** was determined by X-ray diffraction methods (Table 1, Figure 3). For comparison, the crystal structure of **3** was determined and is presented (Table 1, Figure 2). The bond length of Co(1)–Co(2), 2.456 Å, is within the normal range of typical cobalt–cobalt bonds of this kind. In addition, the Co–P bond lengths, 2.266 and 2.2399 Å, show that they are genuine phosphine-to-cobalt dative bonds. The structure of **4a** reveals that the bond distances and angles are within the normal range of typical **4**-like compounds (Table 1, Figure 3).<sup>17a,c</sup> The bond distances are 1.8110, 2.4906, 2.2322, and 2.2343 Å, for P(1)–C(1), Co(1)–Co(2), Co(1)–P(2), and Co(2)–

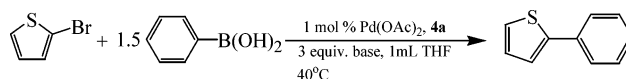
(18) O'Connor, T. J.; Patel, H. A. *Can. J. Chem.* **1971**, *49*, 2706–2711.

**Table 2. Suzuki–Miyaura Coupling Reactions Employing Various **4a**/Pd(OAc)<sub>2</sub> Ratios with KF**

entry <sup>a</sup>	<b>4a</b> /Pd ratio (mol %)	ligand	base	time (h)	yield (%) <sup>b</sup>
1	2:1	<b>4a</b>	3 KF	24	37
2	1:1	<b>4a</b>	3 KF	24	99
3	2:1	<b>4a</b>	3 KF	3	13
4	1.5:1	<b>4a</b>	3 KF	3	30
5	1:1	<b>4a</b>	3 KF	3	85
6	0.5:1	<b>4a</b>	3 KF	3	73
7	0.25:1	<b>4a</b>	3 KF	3	34
8	0:1	<b>4a</b>	3 KF	3	7
9	2:1	<b>5<sup>d</sup></b>	3 KF	3	99
10	1:1	<b>5</b>	3 KF	3	83
11	2:1	<b>5</b>	3 KF	3	98c

<sup>a</sup> Average of two runs. <sup>b</sup> Determined by gas chromatography. <sup>c</sup> Room temperature. See: Wolfe, J. P.; Singer, R. A.; Yang, B. H.; Buchwald, S. L. *J. Am. Chem. Soc.* **1999**, *121*, 9550. <sup>d</sup> 2-(Di-*tert*-butylphosphino)biphenyl **5**.

**Scheme 2** **4a**-Assisted Suzuki–Miyaura Cross-Coupling Reaction



P(3), respectively. As shown, **4a** can be regarded as a phosphine consisting of two bulky substituents, *t*Bu, and one even more bulkier substituent,  $[(\mu\text{-PPh}_2\text{CH}_2\text{PPh}_2)\text{Co}_2(\text{CO})_4][\mu,\eta\text{-PhC}\equiv\text{C}-]$ . Thereby, **4a** provides more acute steric hindrance than the conventional P(*t*Bu)<sub>3</sub>.<sup>19</sup>

**2.2. Suzuki–Miyaura Cross-Coupling Reactions Using Cobalt-Containing Phosphine Ligand **4a** with Pd(OAc)<sub>2</sub>.** Suzuki's coupling reactions were carried out in situ by employing the newly made cobalt-containing palladium complex modified by phosphine ligand **4a** (Table 2). Mostly, the reactions started with 1 molar equiv of 2-bromothiophene, 1.5-fold phenylboronic acid, and 3-fold of KF in 1 mL of THF, and with 1 mol % of **4a**/Pd(OAc)<sub>2</sub> under 40 °C for designated times (Scheme 2).

A low yield, 37%, was obtained when the reaction was conducted with **4a**/Pd(OAc)<sub>2</sub> = 2:1 after 24 h (Table 2, entry 1). To our surprise, rather good yields were observed, even at a low reaction temperature, 40 °C, when the **4a**/Pd(OAc)<sub>2</sub> ratio was changed to 1:1 (Table 2, entries 2, 5). By contrast, the best outcome is always achieved when the **5**/Pd(OAc)<sub>2</sub> ratio is set close to 2 (Table 2, entries 9, 10). To validate this, the efficiencies of the working catalyst with various ratios of ligand/metal were examined. As shown in Table 2, the best result is achieved when the **4a**/Pd(OAc)<sub>2</sub> ratio is 1:1. Therefore, it is concluded that the bonding modes of the active species for the complexes **5**/Pd(OAc)<sub>2</sub> and **4a**/Pd(OAc)<sub>2</sub> are different. As proposed, monophosphine-coordinated complexes Pd(0)L (L = phosphine) might

(19) (a) Littke, A. F.; Fu, G. C. *J. Org. Chem.* **1999**, *64*, 10–11. (b) Littke, A. F.; Fu, G. C. *J. Am. Chem. Soc.* **2001**, *123*, 6989–7000. (c) Littke, A. F.; Fu, G. C. *Angew. Chem., Int. Ed.* **1999**, *38*, 2411–2413. (d) Littke, A. F.; Schwarz, L.; Fu, G. C. *J. Am. Chem. Soc.* **2002**, *124*, 6343–6348. (e) Hundertmark, T.; Littke, A. F.; Buchwald, S. L.; Fu, G. C. *Org. Lett.* **2000**, *2*, 1729–1731. (f) Nishiyama, M.; Yamamoto, T.; Koie, Y. *Tetrahedron Lett.* **1998**, *39*, 617–620. (g) Yamamoto, T.; Nishiyama, M.; Koie, Y. *Tetrahedron Lett.* **1998**, *39*, 2367–2370. (h) Kawatsura, M.; Hartwig, J. F. *J. Am. Chem. Soc.* **1999**, *121*, 1473–1478. (i) Mann, G.; Incarvito, C.; Rheingold, A. L.; Hartwig, J. F. *J. Am. Chem. Soc.* **1999**, *121*, 3224–3225. (j) Hartwig, J. F.; Kawatsura, M.; Hauck, S. I.; Shaughnessy, K. H.; Alcazar-Roman, L. M. *J. Org. Chem.* **1999**, *64*, 5575–5580. (k) Watanabe, M.; Nishiyama, M.; Koie, Y. *Tetrahedron Lett.* **1999**, *40*, 8837–8840. (l) Dai, C.; Fu, G. C. *J. Am. Chem. Soc.* **2001**, *123*, 2719–2724.

**Table 3. Suzuki–Miyaura Coupling Reactions Employing 4a and Various Bases**

entry <sup>a</sup>	Pd/L ratio	ligand	base	time (h)	yield (%) <sup>b</sup>
1	1:1	4a	3 KF	3	85
2	1:1	4a	2 KF	3	79
3	1:1	4a	2 CsF	3	27
4	1:1	4a	2 Na <sub>2</sub> CO <sub>3</sub>	3	14
5	1:1	4a	2 K <sub>2</sub> CO <sub>3</sub>	3	77
6	1:1	4a	2 Cs <sub>2</sub> CO <sub>3</sub>	3	3
7	1:1	4a	2 K <sub>3</sub> PO <sub>4</sub>	3	29
8	1:1	4a	2 NEt <sub>3</sub>	3	7

<sup>a</sup> Average of two runs. <sup>b</sup> Determined by gas chromatography.

be the catalytically active species.<sup>20</sup> It is believed that a three-coordinate palladium complex (Ar)(X)Pd(II)/4a is formed as the active intermediate when a sterically hindered phosphine such as 4a is employed.<sup>21</sup> In the presence of excess ligand 4a, the concentration of the monophosphine complex is decreased, thereby reducing the catalytic efficiency.

As shown experimentally, a well-chosen base/solvent system is crucial for a good performance in the Suzuki–Miyaura reaction.<sup>22</sup> The importance of choosing an appropriate base/solvent system was also well studied theoretically by Ujaque and Maseras et al.<sup>23</sup> It was stated that under the assistance of bases the transmetalation process of organoboronic acid with Ar–Pd(II)–X proceeded more favorably energetically. Table 3 summarizes results from the reactions carried out employing the optimized ligand/metal ratio (4a: Pd(OAc)<sub>2</sub> = 1:1) at 40 °C in 1 mL of THF with a variety of bases. Satisfactory catalytic efficiencies were found while using KF as base. Accordingly, the best efficiency was achieved when the reaction was carried out with 3-fold (rather than 2-fold) KF in THF (entries 1 and 2). Nevertheless, using a large quantity of base always leads to serious solubility and stirring problems. Therefore, 2 equiv of bases was used throughout the rest of the trials (entries 2–8). Note that the catalytic activity in the K<sub>3</sub>PO<sub>4</sub>/THF system could not match its typical performance (entry 7). A rather low yield was also observed in the system where triethylamine was employed as base (entry 8).

Furthermore, the catalytic reactions operating at low loading of the 4a-modified palladium complex were pursued, and the results are shown in Table 4. The reactions were carried out using 2-bromothiophene and phenylboronic acid (entries 1–5) or bromobenzene and phenylboronic acid (entries 6, 7) as substrates and employing the optimized catalytic system (1 mol % 4a/Pd(OAc)<sub>2</sub> = 1:1, 3-fold KF, 1 mL of THF). The yield could reach as high as 91% within 5 h at 40 °C (entry 1). On the other hand, the yield is lowered, 72%, when the

**Table 4. Suzuki–Miyaura Couplings of Arylbromides Employing 4a at Various 4a/Pd Ratios and Reaction Conditions<sup>a</sup>**

entry <sup>b</sup>	Pd/L ratio <sup>c</sup>	temp (°C)	time (h)	yield (%) <sup>d</sup>	TON
1 <sup>e</sup>	1:1	40	5	91	91 (100) <sup>g</sup>
2 <sup>e</sup>	0.5:0.5	40	5	72	144 (200) <sup>g</sup>
3 <sup>e</sup>	0.5:0.5	60	5	99	200 (200) <sup>g</sup>
4 <sup>e</sup>	0.1:0.1	60	5	99	1000 (1000) <sup>g</sup>
5 <sup>e</sup>	0.01:0.01	60	5	3	300 (10 000) <sup>g</sup>
6 <sup>f</sup>	0.01:0.01	60	5	24	2400 (10 000) <sup>g</sup>
7 <sup>f</sup>	0.01:0.01	60	25	41	4100 (10 000) <sup>g</sup>

<sup>a</sup> Reaction conditions (not optimized): 1.0 equiv of arylhalide, 1.5 equiv of phenylboronic acid, and 3 equiv of KF. <sup>b</sup> Average of two runs. <sup>c</sup> Pd/L: mol % Pd to mol % L. <sup>d</sup> Determined by gas chromatography. <sup>e</sup> Product: 2-phenylthiophene. <sup>f</sup> Product: biphenyl. <sup>g</sup> Theoretical TONs.

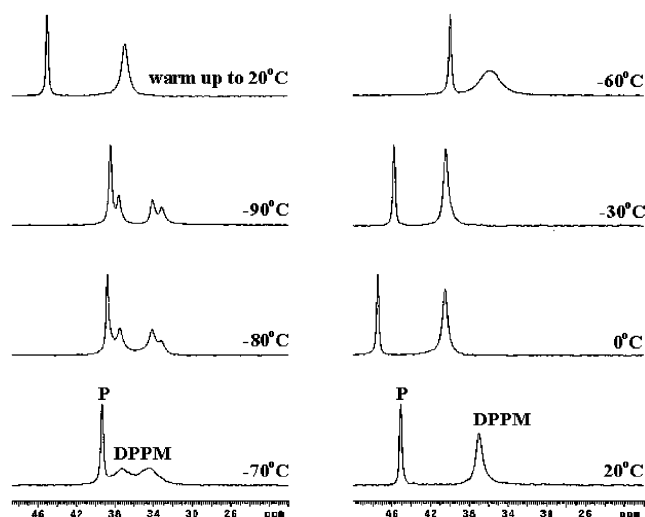


**Figure 4.** Variable-temperature <sup>31</sup>P NMR spectra of 4a in toluene-*d*<sub>8</sub> from 20 to –90 °C.

amount of acting catalyst was reduced to 0.5 mol % (entry 2), and an almost complete conversion was observed when the reaction temperature was raised to 60 °C (entry 3). In addition, high conversion and TONs could be reached at 60 °C even with 0.1 mol % catalyst (entry 4). However, only negligible conversion is detected by GC when the ratio of the catalyst loading was as low as 0.01 mol % (entry 5). The yields were appreciable when bromobenzene, rather than 2-bromothiophene, was used as the reaction substrate (entries 6, 7).

### 2.3. <sup>31</sup>P NMR Studies on 4a and 4a/Pd(OAc)<sub>2</sub>.

#### 2.3.1. DPPM Fluxional Behavior of 4a: Variable-Temperature <sup>31</sup>P NMR of 4a in THF-*d*<sub>8</sub>.

Variable-temperature <sup>31</sup>P NMR experiments of 4a in toluene-*d*<sub>8</sub> were recorded. There was no notable chemical shift variations of the matching signals, –P(*t*Bu)<sub>2</sub> and DPPM, as the temperature was raised from 20 °C to 60 °C. On the other hand, when the measuring temperature was lowered to –60 °C, a broad signal of DPPM was observed (Figure 4). When the probing temperature was fixed at –70 °C, a set of doublet signals of DPPM became apparent. The chemically nonequivalent environments of the two phosphorus atoms, as a result, led to the split of the <sup>31</sup>P NMR peaks. Upon further lowering of the monitoring temperatures to –80 and –90 °C, a set of quartet signals was observed. The observation of the low-temperature NMR spectra is in good agreement

(20) (a) Stambuli, J. P.; Bühl, M.; Hartwig, J. F. *J. Am. Chem. Soc.* **2002**, *124*, 9346–9347. (b) Beare, N. A.; Hartwig, J. F. *J. Org. Chem.* **2002**, *67*, 541–555. (c) Stambuli, J. P.; Stauffer, S. R.; Shaughnessy, K. H.; Hartwig, J. F. *J. Am. Chem. Soc.* **2001**, *123*, 2677–2678. (d) Netherton, M. R.; Fu, G. C. *Org. Lett.* **2001**, *3*, 4295–4298. (e) Aranyos, A.; Old, D. W.; Kiyomori, A.; Wolfe, J. P.; Sadighi, J. P.; Buchwald, S. L. *J. Am. Chem. Soc.* **1999**, *121*, 4369–4378.

(21) (a) Walker, S. D.; Bader, T. E.; Martinelli, J. R.; Buchwald, S. L. *Angew. Chem. Int. Ed.* **2004**, *43*, 1871–1876. (b) Yin, J.; Rainka, M. P.; Zhang, X. X.; Buchwald, S. L. *J. Am. Chem. Soc.* **2002**, *124*, 1162–1163.

(22) Miyaura, N.; Yamada, K.; Sugimoto, H.; Suzuki, A. *J. Am. Chem. Soc.* **1985**, *107*, 972–980.

(23) Braga, A. A.; Morgon, N. H.; Ujaque, G.; Maseras, F. *J. Am. Chem. Soc.* **2005**, *127*, 9298–9307.

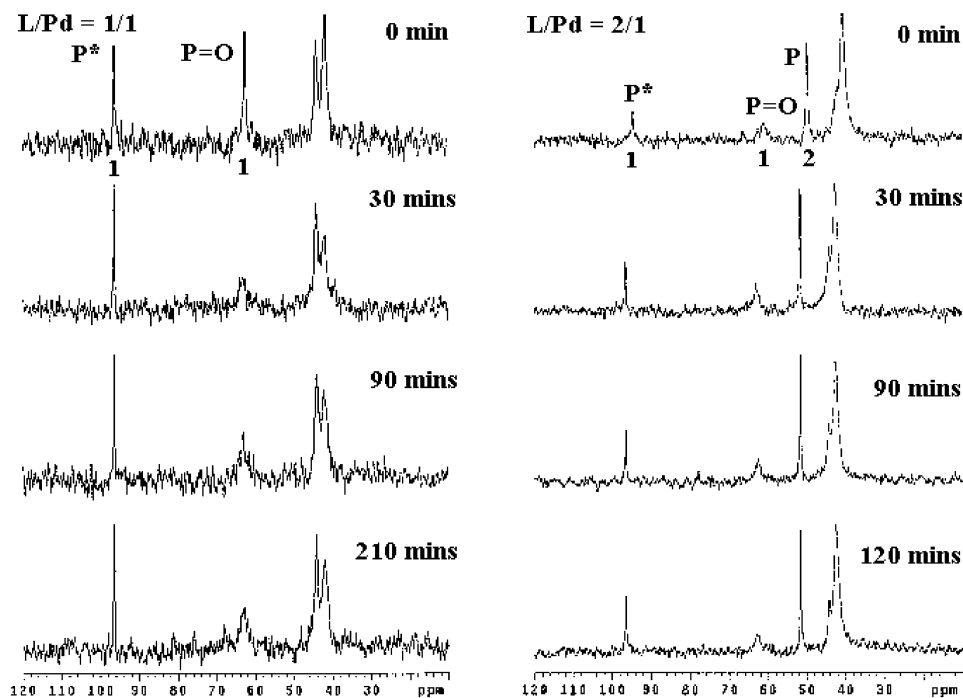
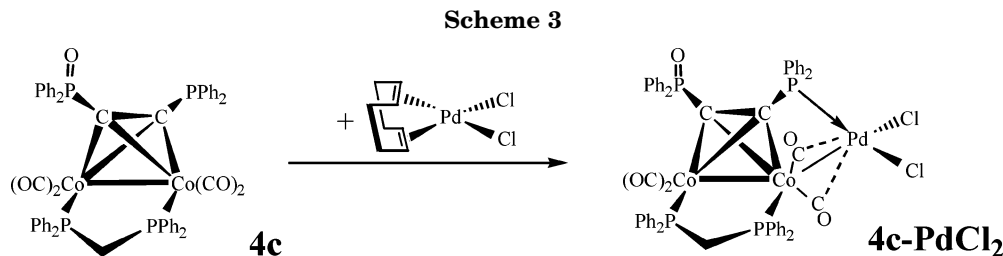


**Figure 5.**  $^{31}\text{P}$  NMR spectra monitored from the reaction of **4a** with  $\text{Pd}(\text{OAc})_2$  in  $\text{THF-}d_8$  at  $40^\circ\text{C}$ . P: **4a**, P=O: **4b**, P\*: unknown. Left:  $\mathbf{4a}/\text{Pd}(\text{OAc})_2 = 1:1$ ; Right:  $\mathbf{4a}/\text{Pd}(\text{OAc})_2 = 2:1$ .



with the low symmetry of the compound revealed in the solid state.

**2.3.2. Reductive Ability of **4a** toward  $\text{Pd}(\text{OAc})_2$  in the Absence of Boronic Acid:  $^{31}\text{P}$  NMR Spectra of  $\mathbf{4a}/\text{Pd}(\text{OAc})_2$  in  $\text{THF-}d_8$ .** It is known that organoboronic acid is a capable reducing agent toward Pd(II) in the Suzuki–Miyaura reaction. Hence, the investigation of the reducing capacity of **4a** toward  $\text{Pd}(\text{OAc})_2$  was carried out in the absence of phenylboronic acid. A sequence of  $^{31}\text{P}$  NMR experiments were conducted at mild temperature,  $40^\circ\text{C}$ , to monitor the conversion of  $\text{Pd}(\text{OAc})_2$  as well as to trace the composition of the plausible acting catalytic species. The spectra were recorded at preselected time intervals after the in situ addition of **4a** to  $\text{Pd}(\text{OAc})_2$  (Figure 5). The initial NMR sample was composed of 0.01 mmol of **4a**,  $\text{Pd}(\text{OAc})_2$ , and 0.5 mL of  $\text{THF-}d_8$ . The whole measurement took 210 min, and the corresponding spectra are shown on the left-hand side of Figure 5 (from the top down). The formation of the oxidized **4b** complex (62.4 ppm) was observed 3 min after the initial mixing. It is believed that Pd(II) was reduced to Pd(0) by **4a**, and the reduction was accompanied with the formation of **4b**. The moderate reducing capacity of phosphine to  $\text{Pd}(\text{OAc})_2$  was demonstrated.<sup>24</sup> A new peak was observed at 96.3 ppm. Its identity is unknown and is tentatively assigned

as **P\***. The composition of **P\*** is proposed as a **4a**-coordinated palladium complex  $(\mathbf{4a})\text{Pd}(0)(\text{OAc})^-$ . Interestingly, the ratio of **P\*/4b** remained 1:1 throughout all the measurements. After 210 min, one more equivalent of **4a** was introduced into the NMR tube. There was no obvious change observed for the ratio of **P\*/4b**. It is noteworthy that the presence of excess **4a** is detected and the integration ratio of **P\*/4b/4a** is 1:1:2. This explains the observation that all the  $\text{Pd}(\text{OAc})_2$  was consumed by the addition of the first batch of **4a** in the earlier stage of the  $^{31}\text{P}$  NMR experiment.

**2.4. Computational Studies of the Modeled Active Species II and  $[\text{II-OAc}]^-$ .** Our previous work has shown that the palladium complex **4c-PdCl<sub>2</sub>** could be prepared from the reaction of a **4a**-like ligand, **4c**, with  $(\text{COD})\text{PdCl}_2$  (Scheme 3). The crystal structure of **4c-PdCl<sub>2</sub>** reveals a unique bonding mode between Pd and **4c**. It leads to the ratio of Pd/ligand = 1:1.<sup>16b</sup> Note that in **4c-PdCl<sub>2</sub>** a direct Co–Pd covalent bond ( $r = 2.6171(5)$  Å) was formed that is joined with a P→Pd dative bond.

It was proposed that either mono- or diphosphine-coordinated Pd(0) species,  $(\text{R}_3\text{P})_n\text{Pd}(0)$  ( $n = 1$  or  $2$ ), could be the major component of the catalytically active species in the phosphine-modified, palladium-catalyzed cross-coupling reactions.<sup>3b,25</sup> Interestingly, a unique  $\pi$ -bonding, which is through  $\eta^1$ - or  $\eta^2$ -arene toward Pd(0) in an  $((\text{aryl})_3\text{P})_n\text{Pd}(0)$  complex, was reported.<sup>25</sup> This

(24) Amatore, C.; Jutand, A. *Acc. Chem. Rev.* **2003**, *33*, 314–321.



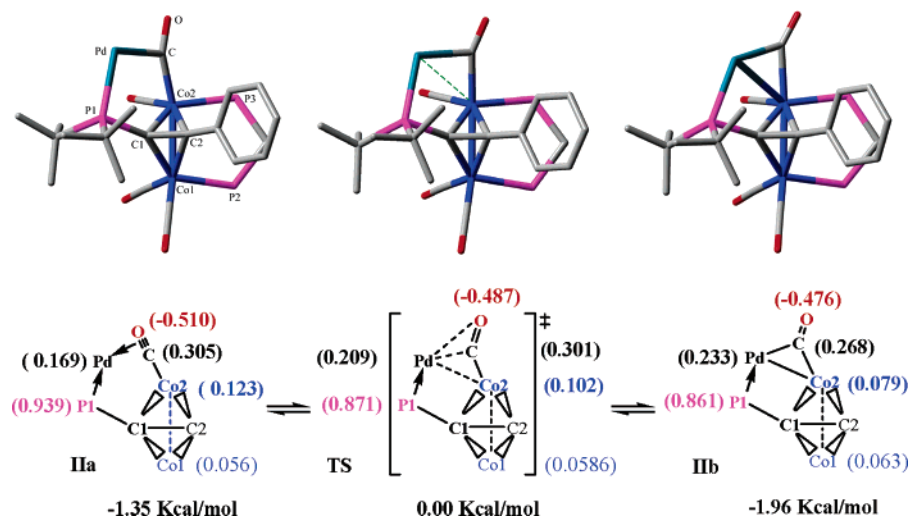


**Figure 6.** B3LYP/631LAN-optimized geometries of compound **IIa**, **TS**, and **IIb**. Energies given are total energies in kcal/mol. Natural charges (NPA) are in parentheses.

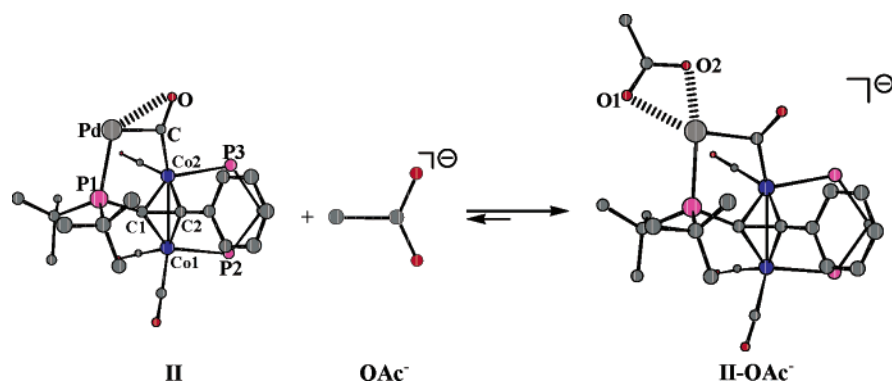


**Figure 7.** B3LYP/631LAN-optimized geometries of compound **II-OAc<sup>-</sup>**, **II**, and **OAc<sup>-</sup>**. The acetate binding energy ( $D^\circ$ ) of **I-OAc<sup>-</sup>** is  $-50.1$  kcal/mol. For optimized geometry of **I-OAc<sup>-</sup>** (in Å): Co1–Co2: 2.507, C–Co2: 1.941, O–Co2: 2.869, P1–Pd: 2.355, C–Pd: 2.025, O–Pd: 2.725, C1–C2: 1.357, O1–Pd: 2.494, O2–Pd: 2.236.

exceptional type of bonding is described as a crucial factor concerning the catalyst's activity and its endurance in the catalytic cycle.<sup>26</sup> Therefore, we are interested in examining the plausible bonding modes of **4a** inside the two potentially active species, **I** and **[I-OAc<sup>-</sup>]**, by theoretical means, since it is difficult to obtain the structural data experimentally. Seeing that the density functional theory (DFT) method, which incorporates electron correlation effects, always provides us with reliable results in the studies of transition metal catalytic reactions,<sup>27</sup> it was employed here to pursue the task.

The computational works employing a simplified mode of **II**, with the four phenyl groups of DPPM of **4a** being replaced by hydrogen atoms, were undertaken. The DFT studies on these two model active species, **II** and **[II-OAc<sup>-</sup>]**, via harmonic vibrational frequency analysis ( $N_{\text{imag}} = 0$ ) have proven them to be local minima at the B3LYP/631LAN level of theory (Figure 6 and Figure 7). Selected optimized bond lengths are

**Table 5.** Selected Bond Lengths (Å) of the Geometrically Optimized **IIa**, **TS**, and **IIb**

	<b>IIa</b>	<b>TS</b>	<b>IIb</b>
Co1–Co2	2.460	2.462	2.474
Pd...Co2	3.295	2.938	2.640
P1–Pd	2.345	2.406	2.422
C–Co2	1.872	1.886	2.009
C–Pd	2.071	2.034	1.986
O–Pd	2.481	2.686	2.933

listed in Table 5. Noteworthy, two stable isomers, **IIa** and **IIb**, with discernible differences in the distances of Pd...Co2 (about 0.655 Å) have been observed. The optimized structure of **IIb** shows that there exists a metal–metal interaction ( $r_{\text{Pd-Co2}} = 2.640$  Å) and a bridge carbonyl group between Pd and Co2 ( $r_{\text{Pd-C}} = 1.990$  Å;  $r_{\text{Co2-C}} = 1.986$  Å;  $r_{\text{Pd-O}} = 2.933$  Å). By contrast, **IIa** shows no Pd...Co2 metal–metal interaction ( $r_{\text{Pd-Co2}} = 3.295$  Å) and there exists a dative bond from a linear  $\mu_2$ -CO to Pd ( $r_{\text{Pd-C}} = 2.071$  Å;  $r_{\text{Pd-O}} = 2.481$  Å;  $r_{\text{Co2-C}} = 1.872$  Å). The species **IIb** is slightly more stable than **IIa** by only 0.6 kcal/mol. The **IIa** ↔ **IIb** isomerization occurs reversibly, through the transition state **TS**, with small energy barrier (1.4 kcal/mol). The proximity of the Pd metal center can be regarded as a hybridization of two bonding modes: one is a terminal linear  $\mu_2$ -CO to Pd dative bond (**IIa**), and the other is a bridge carbonyl ( $\mu_2$ -C≡O) to Pd–Co bond (**IIb**). The changes of bond lengths, lengthening of P1–Pd and O–Pd bonds as well

(25) (a) Faller, J. W.; Sarantopoulos, N. *Organometallics* **2004**, *23*, 2008–2014. (b) Reid, S. M.; Boyle, R. C.; Mauge, J. T.; Fink, M. J. *J. Am. Chem. Soc.* **2003**, *125*, 7816–7817. (c) Yin, J.; Rainka, M. P.; Zhang, X. X.; Buchwald, S. L. *J. Am. Chem. Soc.* **2002**, *124*, 1162–1163. (d) Wolfe, J. P.; Tomori, H.; Sadighi, J. P.; Yin, J.; Buchwald, S. L. *J. Org. Chem.* **2000**, *65*, 1158–1174.

(26) Walker, S. D.; Barder, T. E.; Martinelli, J. R.; Buchwald, S. L. *Angew. Chem., Int. Ed.* **2004**, *43*, 1871–1876.

(27) Null, S.; Hall, M. B. *Chem. Rev.* **2000**, *100*, 353–406.

**Table 6. Wiberg Bond Index (WBI) of the Geometrically Optimized **IIa**, TS, and **IIb****

	<b>IIa</b>	TS	<b>IIb</b>
Co1–Co2	0.276	0.273	0.257
Pd···Co2	0.048	0.347	0.264
P1–Pd	0.440	0.067	0.113

as shortening of Pd–Co2 bond from **IIa** to **IIb**, support this view. Here, one of the cobalt atoms, Co2, and its coordinated carbonyl group in **4a** act as electron donors in **II**. This moiety donates electron density to the zerovalent palladium center. The dicobalt fragment of the metal-containing phosphine **4a** here acts not merely as an irrelevant spectator as in the conventional TM-phosphines mentioned previously but as an active participant. The unique characteristic of **4a** indeed opens a new territory of using metal-containing phosphines as ligands for cross-coupling reactions.

The natural charge<sup>28</sup> for several selected atoms in model compounds **IIa**, TS, and **IIb** provides rather interesting insight into the bonding within molecules (see Figure 6). It reveals that the increase in charges of Co2 and P1 is accompanied with the decrease in charges of Co1 and Pd when the distance of Pd···Co2 becomes closer. This implies that Co1 serves as an electron reservoir that pulls or pushes electron density from or toward the Co2. In **IIb**, the Pd metal receives less from P1, which is due to the formation of a Pd–Co2 interaction. It also shows that the electron densities are pushed from Co1 to the Co2–Pd bond. A similar argument was stated in a theoretical study of the Pauson–Khand reaction by Nakamura et al.<sup>29</sup> One of the cobalt atoms of **4a** provides a Co–Pd interaction, thus stabilizing the Pd(0)L intermediate and providing additional steric hindrance for the metal center. In some respects, this unusual Co–Pd bond mode of **IIb** operates like the  $\pi$ -system of dialkylphenylphosphines mentioned previously.<sup>3b</sup> The  $\pi$ -system of the aromatic ring is able to stabilize the Pd center; nevertheless, it may also lead to cyclo-metalation that will reduce the lifetime of the active species.<sup>5</sup> This commonly observed drawback of arylphosphines should not be a problem in the **4a**/Pd catalytic systems. Moreover, the dissociation process of **OA**<sup>–</sup> from [**II-OAc**]<sup>–</sup> to **II** is unfavorable by 50.1 kcal/mol (Figure 7). This observation echoes Amatore and Jutand's report on the coordination of acetate anion onto the catalytically active Pd(0)PPH<sub>3</sub> species.

The analyses of binding modes of Co1–Co2···Pd within the two intermediates, **IIa** and **IIb**, are of interest to us. The bond orders (WBI)<sup>30</sup> of Co1–Co2, Pd···Co2, and P1–Pd were examined (Table 6). As expected, the bond order of Co1–Co2 becomes lower from **IIa** to **IIb**, while the Pd···Co2 metal–metal interaction becomes stronger (from 0.048 to 0.264). Associated with the variation of metal–metal interactions, the P1–Pd bond order is weaker in **IIb** (0.113) than in **IIa** (0.440). This can be realized by the fact that the increasing interaction of the Pd···Co2 in **IIb** than in **IIa** is observed. The increasing Pd···Co2 interaction will natu-

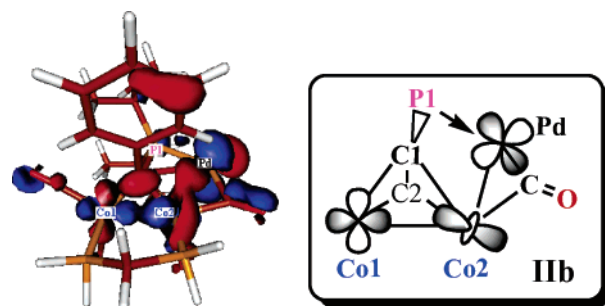


**Figure 8.** Localized Kohn–Sham orbital (B3LYP/6311LAN) of **IIb** (contour intervals: 0.025 in e<sup>–</sup>·au<sup>–3</sup>) and schematic orbital interactions.

rally force part of the electron density from the Co1–Co2 bond to the newly formed Pd···Co2 bond. In this way the electron density donated from P1 will certainly be reduced. A localized molecular orbital (LMO) as depicted in Figure 8 represents the distribution of d-electrons in the three-center bond of Co1–Co2···Pd. The observation of the Co1–Co2···Pd bond from the LMO and the variation of bond orders are in accord with the fact that charges indeed transfer from Co1 to Pd through Co2. Consequently, the dicobalt fragment in **4a** plays an important role as electron reservoir that stabilizes the **4a**-coordinated palladium catalyst.

### 3. Concluding Remarks

We have demonstrated the preparation, characterization, and reactivity studies of a novel cobalt-containing phosphine ligand, **4a**. Preliminary results show that **4a** is an efficient phosphine ligand in Suzuki–Miyaura cross-coupling reactions. Based on both NMR and DFT studies, two **4a**-coordinated palladium compounds, **I** and [**I-OAc**]<sup>–</sup>, are proposed as the active, catalytic species in Suzuki–Miyaura cross-coupling reactions. The formation of Pd···Co interactions and electron density flows among metals in model active species **II** provides a vivid example showing that the dicobalt fragment of the metal-containing phosphine **4a** acts as an electron reservoir in stabilizing the Pd(0) center in the course of the catalytic reaction.

### 4. Experimental Section

**General Procedures.** All operations were performed in a nitrogen-flushed glovebox or in a vacuum system. Freshly distilled solvents were used. All processes for the separation of the products were performed by centrifugal thin layer chromatography (CTLC, Chromatotron, Harrison model 8924). <sup>1</sup>H NMR spectra were recorded (Varian VXR-300S spectrometer) at 300.00 MHz; chemical shifts are reported in ppm relative to deuterated solvent peaks. <sup>31</sup>P and <sup>13</sup>C NMR spectra were recorded at 121.44 and 75.46 MHz, respectively. <sup>1</sup>H NMR spectra of variable-temperature experiments were recorded by the same instrument. Routine <sup>1</sup>H NMR spectra were recorded with a Gemini-200 spectrometer at 200.00 MHz or a Varian-400 spectrometer at 400.00 MHz. IR spectra of the sample powder in KBr were recorded on a Hitachi 270-30 spectrometer. Mass spectra were recorded on a JEOL JMS-SX/SX 102A GC/MS/MS spectrometer. Elemental analyses were recorded on a Heraeus CHN-O-S-Rapid analyzer.

**4.1. Synthesis of PhC≡CP(*t*Bu)<sub>2</sub>, **1**.** The preparative procedures of **1** were modified from the literature.<sup>13</sup> Into a 100 cm<sup>3</sup> round flask were first placed phenylacetylene (2.05 g, 20.00 mmol) and 30 mL of ether. The solution was stirred at

(28) (a) Reed, A. E.; Weinhold, F. *J. Chem. Phys.* **1983**, *78*, 4066–4073. (b) Reed, A. E.; Weinstock, R. B.; Weinhold, F. *J. Chem. Phys.* **1985**, *83*, 735–746.

(29) Yamanaka, M.; Nakamura, E. *J. Am. Chem. Soc.* **2001**, *123*, 1703–1708.

(30) Wiberg, K. B. *Tetrahedron* **1968**, *B*, 1083–1096.



–78 °C before 1.1 molar equiv of *n*-butyllithium (22.0 mmol, 11.0 mL, 2.0 M in cyclohexane) was dropped slowly into the solution. It remained at –78 °C for 2 h before 1.0 molar equiv of di-*tert*-butylchlorophosphine (3.61 g, 20.00 mmol), dissolved in 4 mL of ether, was added slowly into the solution. The reaction mixture was then allowed to warm to room temperature and then stirred again for the next 4 days. Later, the solvent was removed under reduced pressure and then toluene was added to precipitate the lithium chloride. After filtration, the resulting solution was further purified through flash chromatography. A white solid was obtained and identified as **1** in a yield of 80.0% (3.92 g, 15.91 mmol). A similar quantity of product was obtained as reported previously by the literature.<sup>31</sup>

**1**: <sup>1</sup>H NMR (CDCl<sub>3</sub>, δ/ppm) 7.48–7.45(m, 2H, arene), 7.32–7.30(m, 3H, arene), 1.30(d, *J*<sub>P–H</sub> = 12.6 Hz, 18H, *t*Bu); <sup>13</sup>C NMR (CDCl<sub>3</sub>, δ/ppm) 131.4(s, 2C, meta-position of arene), 128.1(s, 2C, ortho-position of arene), 123.6(s, 1C, para-position of arene), 105.5(d, *J*<sub>P–H</sub> = 2.3 Hz, 1C, ipso-position of arene), 88.1(d, *J*<sub>P–H</sub> = 20.4 Hz, 1C, PC≡C), 32.8(d, *J*<sub>P–H</sub> = 16.1 Hz, 2C, –C(CH<sub>3</sub>)<sub>3</sub>), 29.6(d, *J*<sub>P–H</sub> = 14.5 Hz, 6C, –C(CH<sub>3</sub>)<sub>3</sub>); <sup>31</sup>P NMR (CDCl<sub>3</sub>, δ/ppm) 12.2(s, 1P, C≡CP); IR (KBr, cm<sup>–1</sup>) 2176(m, C≡C). Anal. Calcd: C, 78.01; H, 9.41. Found: C, 77.4; H, 9.30. MS(FAB) *m/z* = 246.0(P<sup>+</sup>).

**4.2. Synthesis of PhC≡CP(=O)(*t*Bu)<sub>2</sub>, 2.** The title compound was prepared according to the literature procedures.<sup>32</sup> Into a 100 cm<sup>3</sup> round flask were placed 5.00 mmol of **1** (1.23 g) and 15 mL of THF. At 0 °C, 1.5 mL of 30% H<sub>2</sub>O<sub>2</sub> was added to the solution drop-by-drop, and then the mixture was stirred for 30 min. The reaction temperature was raised to 25 °C and stirred for another 2 h. The mixture was poured into a separatory funnel with 25 mL of CH<sub>2</sub>Cl<sub>2</sub> and 10 mL of water. Later, the organic layer was collected, dried with MgSO<sub>4</sub>, filtered through silica gel, and concentrated under reduced pressure. A pale yellow solid was identified as the title compound and produced in quantitative yield.

**2**: <sup>1</sup>H NMR (CDCl<sub>3</sub>, δ/ppm) 7.54–7.52(m, 2H, arene), 7.44–7.34(m, 3H, arene), 1.38(d, *J*<sub>P–H</sub> = 14.8 Hz, 18H, *t*Bu); <sup>13</sup>C NMR (CDCl<sub>3</sub>, δ/ppm) 132.3(s, 2C, meta-position of arene), 130.2(s, 2C, ortho-position of arene), 128.5(s, 1C, para-position of arene), 120.4(d, *J*<sub>P–H</sub> = 3.7 Hz, 1C, ipso-position of arene), 103.3(d, *J*<sub>P–H</sub> = 20.1 Hz, 1C, P(=O)C≡C), 81.2(d, *J*<sub>P–H</sub> = 128.8 Hz, 1C, C≡CP(=O)), 36.2(d, *J*<sub>P–H</sub> = 72.0 Hz, 2C, –C(CH<sub>3</sub>)<sub>3</sub>), 26.3(s, 6C, –C(CH<sub>3</sub>)<sub>3</sub>); <sup>31</sup>P NMR (CDCl<sub>3</sub>, δ/ppm) 44.7(s, 1P, C≡CP); IR (KBr, cm<sup>–1</sup>) 2180 (m, C≡C). Anal. Calcd: C, 73.26; H, 8.84. Found: C, 72.95; H, 8.48. MS(FAB) *m/z* = 263.0 (P<sup>+</sup> + 1).

**4.3. Synthesis of (μ-PPh<sub>2</sub>CH<sub>2</sub>PPh<sub>2</sub>)Co<sub>2</sub>(CO)<sub>6</sub>, 3.**<sup>33</sup> A 100 cm<sup>3</sup> flask was charged with 1.00 mmol of dicobalt octacarbonyl, Co<sub>2</sub>(CO)<sub>8</sub> (0.34 g), 1 molar equiv of DPPM (0.39 g), and 10 mL of toluene. The solution was stirred at 65 °C for 4 h and gave a major product, a yellow-colored, biphosphino-coordinated (μ-PPh<sub>2</sub>CH<sub>2</sub>PPh<sub>2</sub>)Co<sub>2</sub>(CO)<sub>6</sub>, and a trace amount of green-colored, monophosphino-coordinated (Ph<sub>2</sub>CH<sub>2</sub>PPh<sub>2</sub>)Co<sub>2</sub>(CO)<sub>7</sub>. Without further separation, the reaction mixture was used in the succeeding reactions. Also, suitable crystals of **3** were obtained from the mixture solvent system (CH<sub>2</sub>Cl<sub>2</sub>/hexane = 1:1) at 4 °C, and its structure was determined by the X-ray diffraction method.

**4.4. Synthesis of [(μ-PPh<sub>2</sub>CH<sub>2</sub>PPh<sub>2</sub>)Co<sub>2</sub>(CO)<sub>4</sub>][μ,η-PhC≡CP(*t*Bu)<sub>2</sub>], 4a, and [(μ-PPh<sub>2</sub>CH<sub>2</sub>PPh<sub>2</sub>)Co<sub>2</sub>(CO)<sub>4</sub>][μ,η-PhC≡CP(*t*Bu)<sub>2</sub>], 4b.** Compound **3** was prepared by the procedures as shown in section 4.3. Without further separation, the reaction flask was charged with 1 molar equiv of **1** (0.246 g), in 5 mL of toluene, and then the mixture was allowed to stir at 65 °C for 1 h. This was followed by reacting at 110 °C for

another 16 h. The solvent was removed under reduced pressure, and the resulting dark red residue was subjected to purification by CTLC chromatography. The first band, dark red in color, was eluted out by mixed solvent (CH<sub>2</sub>Cl<sub>2</sub>:hexane = 1:3) and was identified as **4a** in a yield of 72.0% (0.62 g, 0.72 mmol). Then, the second band, red-colored, was eluted out by mixed solvent (EA:CH<sub>2</sub>Cl<sub>2</sub> = 1:10) and was identified as **4b** in a yield of 27.0% (0.24 g, 0.27 mmol). Interestingly, **4a** exhibits a dark red band in the CTLC plate and blackish green in solution.

Compound **4b** can also be prepared directly from the reaction of **3** and **2**. As mentioned, a mixture containing mostly **3** was prepared according to the procedures shown in section 4.3. Without further separation, the reaction flask was charged with 1 molar equiv of compound **2** (0.26 g), which was dissolved in 5 mL of toluene. The mixed solution was then allowed to react at 85 °C for 20 h before the solvent was removed under reduced pressure. The resulting red-colored residue was subjected to purification by CTLC chromatography. The only red band was eluted out by mixed solvent (EA:CH<sub>2</sub>Cl<sub>2</sub> = 1:10). It was identified as **4b** and was produced in quantitative yield (0.88 g, 1.00 mmol).

**4a**: <sup>1</sup>H NMR (CDCl<sub>3</sub>, δ/ppm) 7.92–6.94(m, 25H, arene), 3.31(m, 1H, DPPM), 3.03(m, 1H, DPPM), 1.60(d, *J*<sub>P–H</sub> = 17.1 Hz, *t*Bu, #1), 1.26(d, *J*<sub>P–H</sub> = 10.8 Hz, *t*Bu, #2); <sup>13</sup>C NMR (CDCl<sub>3</sub>, δ/ppm) 132.48–128.52(30C, arenes), 30.5(d, *J*<sub>P–C</sub> = 12.1 Hz, 3C, –C(CH<sub>3</sub>)<sub>3</sub>), 28.15(s, 6C, –C(CH<sub>3</sub>)<sub>3</sub>); <sup>31</sup>P NMR (CDCl<sub>3</sub>, δ/ppm) 113.9(s, 1P, C≡CP, #1), 44.3(s, 1P, C≡CP, #2), 37.0(s, 2P, DPPM, #2), 34.8(s, 2P, DPPM, #1); IR (KBr, cm<sup>–1</sup>) 2020(s), 1994(s), 1966(s) (COs). Anal. Calcd: C, 62.80; H, 5.27. Found: C, 60.83; H, 5.72. MS(FAB) *m/z* = 861.0 (P<sup>+</sup>).

**4b**: <sup>1</sup>H NMR (CDCl<sub>3</sub>, δ/ppm) 7.55–7.02(m, 25 H, arene), 3.53(m, 1H, DPPM), 3.24(m, 1H, DPPM), 1.42(d, *J*<sub>P–H</sub> = 13.8 Hz, 18H, *t*Bu); <sup>13</sup>C NMR (CDCl<sub>3</sub>, δ/ppm) 206.26(s, 2C, COs), 201.67(s, 2C, COs), 143.03–125.77(30C, arenes), 110.21(s, 1C, PC≡), 65.79(1C PhC≡), 38.11(d, *J*<sub>P–C</sub> = 62.9 Hz, 1C, –C(CH<sub>3</sub>)<sub>3</sub>), 33.51(t, *J*<sub>P–C</sub> = 21.4 Hz, 1C, –CH<sub>2</sub> of DPPM), 28.11(s, 3C, –C(CH<sub>3</sub>)<sub>3</sub>); <sup>31</sup>P NMR (CDCl<sub>3</sub>, δ/ppm) 59.1(s, 1 P, C≡C(P=O)), 36.3(s, 2 P, DPPM); IR (KBr, cm<sup>–1</sup>) 2025(s), 1998(s), 1968(s) (COs). Anal. Calcd: C, 73.26; H, 8.84. Found: C, 72.0; H, 8.57. MS(FAB) *m/z* = 876.7 (P<sup>+</sup>).

**4.5. General Procedures for the Suzuki–Miyaura Cross-Coupling Reaction and Characterization of Products.** The Suzuki–Miyaura coupling reaction was performed according to Buchwald's procedures.<sup>3d</sup> Normally, the ratio of the palladium source, Pd(OAc)<sub>2</sub>, to the reacting substances is around 1%, while the ratio of **4a**:Pd(OAc)<sub>2</sub> ranges from 2:1 to 0:1 depending on the reaction conditions executed. The generalized procedures are shown as follows. A suitable oven-dried Schlenk flask, which was previously evacuated and backfilled with nitrogen, was charged with Pd(OAc)<sub>2</sub> (2.20 mg, 0.01 mmol), 2–0-fold **4a**, 1.5-fold boronic acid (0.18 g, 1.50 mmol), and 2- or 3-fold bases. Then, 1 mL of THF and 1.00 mmol of aryl halide were added. The flask was then sealed with a Teflon screw cap, and the reaction mixture was heated to 40 or 60 °C depending on the reaction requirements. Subsequently, HCl(aq) (2.3 M, 10 mL) was added to the resulting solution and the reaction was quenched. The organic layer was extracted with CH<sub>2</sub>Cl<sub>2</sub> (10 mL × 3). Then, the combined organic layer was dried over anhydrous magnesium sulfate, filtered, and concentrated with a rotary evaporator. The crude material was passed quickly through a small column of silica gel to get rid of solid impurities. Then, the residue was dissolved in a 10 mL of toluene solution with naphthalene as the internal standard. The final yield was calibrated and determined by gas chromatography.

**4.6. Experimental Methods for NMR Studies. Variable-Temperature <sup>31</sup>P NMR of 4a in THF-*d*<sub>8</sub>.** A suitable amount of **4a** was first dissolved in THF-*d*<sub>8</sub> and then was placed in a sealed NMR tube. The spectra were monitored and recorded

(31) Empsall, H. D.; Hyde, E. M.; Mentzer, E.; Shaw, B. L. *J. Chem. Soc. Dalton Trans.* **1977**, 2285–2291.

(32) Liu, B.; Wang, K. K.; Peterson, J. L. *J. Org. Chem.* **1996**, *61*, 8503–8507.

in a 300 MHz NMR spectrometer over the designated temperatures and time intervals.

**4.7. Computational Details.** Calculations reported in this study were performed via density functional theory<sup>34</sup> using the Gaussian03<sup>35</sup> series of packages. To make the computations feasible, the size-reduced model compound with four phenyl groups of DPPM of **4a** being replaced by four hydrogen atoms was employed. Geometries were optimized at the B3LYP/631LAN level of theory,<sup>36</sup> in which the LANL2DZ including the double- $\zeta$  basis set for the valence and outermost core orbitals combined with a pseudopotential was used for Co and Pd,<sup>37</sup> while the 6-31G(d) basis set was used for the other atoms. All the optimized geometries were minima and verified by the harmonic vibrational frequency analysis, which was obtained via analytical energy second derivatives. All the stationary points found were characterized via harmonic vibrational frequency analysis as minima and transition states. IRC<sup>33</sup> analyses follow the geometry optimization to ensure the transition structures are smoothly connected by two proximal minima along the reaction coordinate. Natural charges<sup>28</sup> and Wiberg bond indices<sup>30</sup> were evaluated with Weinhold's NBO method.<sup>38</sup> Localized Kohn–Sham orbitals (LMO)<sup>39</sup> were obtained by Boys' localization procedure from the occupied B3LYP/631LAN Kohn–Sham orbitals based on the B3LYP/

631LAN-optimized geometries. The wave functions were analyzed with MOLDEN<sup>40</sup> to plot electron density contours and visualize the IR eigenvectors.

**4.8. X-ray Crystallographic Studies.** Suitable crystals of **3** and **4a** were sealed in thin-walled glass capillaries under a nitrogen atmosphere and mounted on a Bruker AXS SMART 1000 diffractometer. Intensity data were collected in 1350 frames with increasing width (0.3° per frame). The absorption correction was based on the symmetry equivalent reflections using the SADABS program. The space group determination was based on a check of the Laue symmetry and systematic absences and was confirmed using the structure solution. The structure was solved by direct methods using the SHELXTL package.<sup>41</sup> All non-H atoms were located from successive Fourier maps, and hydrogen atoms were refined using a riding model. Anisotropic thermal parameters were used for all non-H atoms, and fixed isotropic parameters were used for H atoms.<sup>42</sup> Crystallographic data of **3** and **4a** are summarized in Table 1.

Crystallographic data for the structural analysis have been deposited with the Cambridge Crystallographic Data Center, CCDC nos. 260502 and 260503 for compounds **3** and **4a**, respectively. Copies of this information may be obtained free of charge from the Director, CCDC, 12 Union Road, Cambridge CB2 1EZ, UK (fax: +44-1223-336033; e-mail: deposit@ccdc.cam.ac.uk or www: <http://www.ccdc.cam.ac.uk>).

**Acknowledgment.** We are grateful to the National Science Council of the R.O.C. (Grant NSC 93-2113-M-005-020) for financial support. Excellent service and generous computational quota were provided by National Center for High-Performance Computing (NCHC).

**Supporting Information Available:** Figures and tables of the geometry determined from both X-ray crystallographic determination, **4a**, and B3LYP/631LAN calculations, **4A**, tables of energies in hartrees, and optimized structures of model compounds **IIa**, **TS**, **IIb**, [**IIa-OAc**<sup>-</sup>], and **4A** are available.

OM050060J

(39) (a) Boys, S. F.; *Quantum Theory of Atoms, Molecules, and Solid State*; Lowdin, P. O., Ed.; Academic Press: New York, 1968; pp 235–262. (b) Haddon, R. C.; Williams, G. R. *J. Chem. Phys. Lett.* **1976**, *42*, 453–455. (c) Kohn, W.; Sham, L. *J. Phys. Rev.* **1965**, *140*, A1133–1138.

(40) Schaftenaar, G.; Noordik, J. H. *J. Comput.-Aided Mol. Des.* **2000**, *14*, 123–134.

(41) Sheldrick, G. M. *SHELXTL PLUS User's Manual*, Revision 4.1; Nicolet XRD Corporation: Madison, WI, 1991.

(42) The hydrogen atoms were set to ride on carbon or oxygen atoms in their idealized positions and held fixed with the C–H distances of 0.96Å.

(33) (a) Hohenberg, P.; Kohn, W. *Phys. Rev.* **1964**, *136*, B864. (b) Kohn, W.; Sham, L. *J. Phys. Rev.* **1965**, *140*, A1133. (c) Parr, R. G.; Yang, W. *Density-functional theory of atoms and molecules*; Oxford University Press: Oxford, 1989.

(34) Frisch, M. J.; Trucks, G. W.; Schlegel, H. B.; Scuseria, G. E.; Robb, M. A.; Cheeseman, J. R.; Montgomery, Jr., J. A.; Vreven, T.; Kudin, K. N.; Burant, J. C.; Millam, J. M.; Iyengar, S. S.; Tomasi, J.; Barone, V.; Mennucci, B.; Cossi, M.; Scalmani, G.; Rega, N.; Petersson, G. A.; Nakatsuji, H.; Hada, M.; Ehara, M.; Toyota, K.; Fukuda, R.; Hasegawa, J.; Ishida, M.; Nakajima, T.; Honda, Y.; Kitao, O.; Nakai, H.; Klene, M.; Li, X.; Knox, J. E.; Hratchian, H. P.; Cross, J. B.; Bakken, V.; Adamo, C.; Jaramillo, J.; Gomperts, R.; Stratmann, R. E.; Yazyev, O.; Austin, A. J.; Cammi, R.; Pomelli, C.; Ochterski, J. W.; Ayala, P. Y.; Morokuma, K.; Voth, G. A.; Salvador, P.; Dannenberg, J. J.; Zakrzewski, V. G.; Dapprich, S.; Daniels, A. D.; Strain, M. C.; Farkas, O.; Malick, D. K.; Rabuck, A. D.; Raghavachari, K.; Foresman, J. B.; Ortiz, J. V.; Cui, Q.; Baboul, A. G.; Clifford, S.; Cioslowski, J.; Stefanov, B. B.; Liu, G.; Liashenko, A.; Piskorz, P.; Komaromi, I.; Martin, R. L.; Fox, D. J.; Keith, T.; Al-Laham, M. A.; Peng, C. Y.; Nanayakkara, A.; Challacombe, M.; Gill, P. M. W.; Johnson, B.; Chen, W.; Wong, M. W.; Gonzalez, C.; and Pople, J. A. *Gaussian 03*, Revision B.04; Gaussian, Inc.: Wallingford, CT, 2004.

(35) (a) Becke, A. D. *J. Chem. Phys.* **1993**, *98*, 5648–5652. (b) Lee, C.; Yang, W.; Parr, R. G. *Phys. Rev. B* **1988**, *37*, 785–789.

(36) (a) Hay, P. J.; Wadt, W. R. *J. Chem. Phys.* **1985**, *82*, 270–283. (b) Wadt, W. R.; Hay, P. J. *J. Chem. Phys.* **1985**, *82*, 284–298. (c) Hay, P. J.; Wadt, W. R. *J. Chem. Phys.* **1985**, *82*, 299–310.

(37) Lisic, E. C.; Hanson, B. E. *Inorg. Chem.* **1986**, *25*, 812–815.

(38) Reed, A. E.; Curtiss, L. A.; Weinhold, F. *Chem. Rev.* **1988**, *88*, 899–926.